ORIGINAL ARTICLE

JBMR®

Combined Collagen-Induced Arthritis and Organic Dust-Induced Airway Inflammation to Model Inflammatory Lung Disease in Rheumatoid Arthritis

Jill A Poole,[1]* Geoffrey M Thiele,[2,3] Katherine Janike,[1] Amy J Nelson,[1] Michael J Duryee,[2,3] Kathryn Rentfro,[1] Bryant R England,[2,3] Debra J Romberger,[1,2] Joseph M Carrington,[1] Dong Wang,[4] Benjamin J Swanson,[5] Lynell W Klassen,[2,3] and Ted R Mikuls[2,3]

[1]Pulmonary, Critical Care, Sleep & Allergy Division, Department of Internal Medicine, University of Nebraska Medical Center, Omaha, NE, USA
[2]Veterans Affairs Nebraska-Western Iowa Health Care System, Research Service, Omaha, NE, USA
[3]Rheumatology Division, Department of Internal Medicine, University of Nebraska Medical Center, Omaha, NE, USA
[4]Pharmaceutical Sciences, University of Nebraska Medical Center, Omaha, NE, USA
[5]Pathology and Microbiology Department, University of Nebraska Medical Center, Omaha, NE, USA

ABSTRACT

Rheumatoid arthritis (RA) is characterized by extra-articular involvement including lung disease, yet the mechanisms linking the two conditions are poorly understood. The collagen-induced arthritis (CIA) model was combined with the organic dust extract (ODE) airway inflammatory model to assess bone/joint–lung inflammatory outcomes. DBA/1J mice were intranasally treated with saline or ODE daily for 5 weeks. CIA was induced on days 1 and 21. Treatment groups included sham (saline injection/saline inhalation), CIA (CIA/saline), ODE (saline/ODE), and CIA + ODE (CIA/ODE). Arthritis inflammatory scores, bones, bronchoalveolar lavage fluid, lung tissues, and serum were assessed. In DBA/1J male mice, arthritis was increased in CIA + ODE > CIA > ODE versus sham. Micro-computed tomography (μCT) demonstrated that loss of BMD and volume and deterioration of bone microarchitecture was greatest in CIA + ODE. However, ODE-induced airway neutrophil influx and inflammatory cytokine/chemokine levels in lavage fluids were increased in ODE > CIA + ODE versus sham. Activated lung $CD11c^{+}CD11b^{+}$ macrophages were increased in ODE > CIA + ODE > CIA pattern, whereas lung hyaluronan, fibronectin, and amphiregulin levels were greatest in CIA + ODE. Serum autoantibody and inflammatory marker concentrations varied among experimental groups. Compared with male mice, female mice showed less articular and pulmonary disease. The interaction of inhalation-induced airway inflammation and arthritis induction resulted in compartmentalized responses with the greatest degree of arthritis and bone loss in male mice with combined exposures. Data also support suppression of the lung inflammatory response, but increases in extracellular matrix protein deposition/interstitial disease in the setting of arthritis. This coexposure model could be exploited to better understand and treat RA–lung disease. © 2019 American Society for Bone and Mineral Research.

KEY WORDS: RHEUMATOID ARTHRITIS; INTERSTITIAL LUNG DISEASE; INFLAMMATION; COEXPOSURE; AUTOIMMUNITY

Introduction

Rheumatoid arthritis (RA) is a debilitating autoimmune disease that is often associated with a number of comorbidities including interstitial lung disease (ILD), chronic bronchitis, chronic obstructive pulmonary disease (COPD), pulmonary nodules, and pleural diseases.[1] Respiratory-related deaths are the most overrepresented cause of death in men and women with RA.[2,3] Whereas symptomatic ILD occurs in up to 10% to 15% of RA patients and is a well-established extra-articular manifestation associated with a poor long-term prognosis,[4–6] COPD is the most common cause of respiratory-related deaths.[2,3,7] The importance of the relationship between arthritis and lung inflammation has been further strengthened with evidence linking RA autoantibody generation to the respiratory mucosa because individuals with chronic lung disease appear to produce characteristic RA autoantibodies, even in the absence of RA.[8–12] Correspondingly, RA patients with comorbid lung disease have increased RA disease activity and higher anticyclic citrullinated peptide (anti-CCP) antibody concentrations.[13,14]

Several inhalant environmental factors are implicated in the development of RA with cigarette smoking being the most well-established risk factor.[15,16] Occupational inhalant exposures have been increasingly associated with the risk of disease development, particularly among males.[17] Elevated risks of RA

Received in original form January 4, 2019; revised form March 15, 2019; accepted April 3, 2019. Accepted manuscript online June 24, 2019.
Address correspondence to: Jill A Poole, MD, 985900 Nebraska Medical Center, Omaha, NE 68198. E-mail: japoole@unmc.edu
Additional Supporting Information may be found in the online version of this article.
Journal of Bone and Mineral Research, Vol. 34, No. 9, September 2019, pp. 1733–1743
DOI: 10.1002/jbmr.3745

have been mainly observed among men who are farmers, mechanics, construction workers, and warehouse workers, in addition to those with occupational exposure to silica.[17–19] Among women, the link between occupational exposures and RA risk has been less clear.[17] These observations support the hypothesis that repetitive inhalation exposure to an inflammatory environmental insult could precipitate and/or potentiate arthritis, particularly in men. However, the mechanisms linking pulmonary inflammation to arthritis development remain poorly understood. Development of such an animal model would be advantageous to understand mechanisms of disease and explore potential interventional strategies.

Animal modeling of arthritis–lung disease interactions are limited; however, studies have been performed using the arthritic SKG mouse model whereby the arthritis-prone SKG mice develop a cellular and fibrotic interstitial pneumonia.[20] The limitation of this model is that the SKG mice do not develop autoimmunity or arthritis following inhalation injury (ie, tobacco smoke or bleomycin), which had been interpreted to suggest that lung injury/inflammation alone is not sufficient to induce arthritis.[20] In our established animal model (C57BL/6 strain) of agriculture-related organic dust extract (ODE) exposure-induced airway inflammatory disease,[21] we recently discovered evidence that ODE induced citrullinated and malondialdehyde-acetaldehyde- (MAA-) modified lung proteins with associated systemic autoantibody responses.[22] This is relevant because anticitrullinated protein antibody (ACPA) and anti-MAA antibody responses have been shown to characterize RA.[1,23] Organic dusts are complex, comprised of particulates, trace metals, and enriched with gram-negative and gram-positive microbial components that elicit a strong lung inflammatory response marked by neutrophil influx and cytokine release.[24,25] Whereas agriculture work exposures are strongly associated with the development of inflammatory lung diseases including chronic bronchitis, COPD, and non-allergic asthma, RA has also been found to be increased in farmers.[26–28]

Thus, the objective of this study was to combine the ODE-induced airway inflammatory model with the collagen-induced arthritis (CIA) model in arthritis-susceptible mice (ie, DBA/1J strain) to establish a new paradigm by which to study the interplay of lung and joint inflammation in RA.

Materials and Methods

Animals

Animal procedures were approved by our Institutional Animal Care and Use Committee (University of Nebraska Medical Center, Omaha, NE, USA) and were conducted in accordance with the U.S. Public Health Service Policy for the Humane Care and Use of Laboratory Animals; the USDA and the Animal Welfare Act; the U.S. Government Principles for the Utilization and Care of Vertebrate Animals Used in Testing, Research and Training; the National Research Council of the National Academies Guide for the Care and Use of Laboratory Animals (aka, The Guide); and all local guidelines and policies.

DBA/1J strain mice betweensix to 8 weeks of age were purchased from the Jackson Laboratory (Bar Harbor, ME, USA). Male mice were utilized for all initial studies shown, and separate studies with female mice were also conducted. DBA/1J mice were group housed and fed alfalfa-free chow *ad libitum* (Envigo Teklad, Huntingdon, Cambridgeshire, UK) as recommended by the mouse vendor, the Jackson Laboratory. Mice were housed in a specific pathogen-free facility employing 12-hour light and dark cycles. The University of Nebraska Medical Center animal facilities are accredited by the Association for Assessment and Accreditation of Laboratory Animal Care International and are supervised by three doctors of veterinary medicine.

Organic dust extract

Aqueous organic dust extract (ODE) was prepared from swine confinement feeding facilities as previously described.[21] Briefly, dust (1 g) was incubated in sterile Hank's Balanced Salt Solution (10 mL; Mediatech, Manassas, VA, USA) for 1 hour and centrifuged for 30 minutes at 2850*g* and repeated. The final supernate was filter-sterilized (0.22 μm) to remove microorganisms and coarse particles. Endotoxin concentrations in 100% ODE ranged from 1200 to 1400 EU/mL as determined using the limulus amebocyte lysate assay (Lonza, Walkersville, MD, USA). Muramic acid levels (bacterial cell wall peptidoglycans) were previously determined by mass spectrometry to be approximately 70 ng/mg.[29] Stock ODE was batch prepared and stored at −20˚C; aliquots were diluted for each experiment to a final concentration (vol/vol) of 12.5% in sterile PBS (pH 7.4; diluent). ODE 12.5% has been shown to elicit optimal experimental outcomes and is well-tolerated.[21]

Animal coexposure model

Mice were randomized to one of four treatment groups: sham (saline injection/saline inhalation), collagen-induced arthritis (CIA; CIA injection/saline inhalation), ODE (saline injection/ODE inhalation), and CIA + ODE (CIA injection/ODE inhalation). CIA was induced as per Chondrex protocol (Chondrex; Redmond, WA, USA). Briefly, 2 mg/mL of chick type II collagen emulsified in Freund's complete adjuvant (FCA) was injected subcutaneously on day 1 at a final concentration of 100 μg and again at week 3, using chicken collagen emulsified in Freund's incomplete adjuvant (IFA). Sham injections were conducted with PBS. Airway inflammatory disease was induced using an established intranasal inhalation repetitive exposure animal model,[21] whereby mice received daily treatment with either 50 μL of sterile saline or 12.5% ODE daily for 5 weeks (weekends excluded). Animals were euthanized 5 hours following the final exposure. Investigators were not blinded during allocation, animal handling, and endpoint measurements.

Arthritis evaluation

Mice were assessed weekly for the development of arthritis using the semiquantitative, mouse arthritis scoring system provided by Chondrex (www.chondrex.com). This protocol is based on hind-foot examination with a range of 0 (no inflammation) to 4 (erythema and severe swelling encompassing ankle, foot, and digits).

Bone micro-computed tomography

In our previous studies,[30,31] we have shown that the response to injection with citrullinated proteins results in little or no arthritis, but an increase in bone loss. Thus, in the present study, we chose to use high-resolution μCT of the trabecular

bone in the tibia and calcaneus to assess the effects of CIA, ODE, and coexposure on systemic bone quantity and quality. Following euthanization, hind limbs (calcaneus and tibia) were isolated and processed for μCT scanning and analysis.[32] Bones were scanned using high-resolution μCT (Skyscan 1172; Bruker, Kontich, Belgium) with bone position corrected using Dataviewer (Skyscan) to assure proper orientation.[33] For tibias, resolution was acquired at 6.07 μm, the X-ray source set at 48 kV and 187 μA, and scanning was done at 0.4-degree intervals with four average frames/rotation. NRECON (Skyscan) software (version 1.7.1.6, April 2017) was used to reconstruct scanned images. Analysis of the reconstructed tibia images was undertaken using CTAn (Skyscan) software with final analysis conducted on a volume of interest of trabecular bone (2.5-mm distance; 2500/5.97; 419 slices) in the metaphyseal region. For ankles, we set a resolution of 4.78 μm at 0.4-degree intervals with six average frames, and the X-ray source set at 59 kV and 167 uA and a starting position of 50 slices from growth plate with 75 slices deep. Bone-quality parameters, including BMD (g/cm^3), bone volume-to-tissue volume ratio, bone surface to bone volume ratio, trabecular number, trabecular separation, trabecular pattern factor, trabecular thickness, and polar moment of inertia, were calculated.[34,35]

Bronchoalveolar lavage fluid cell analysis

Bronchoalveolar lavage fluid (BALF) was collected using 3×1 mL PBS. Total cell numbers from the combined recovered lavage were enumerated and differential cell counts determined from cytospin-prepared slides (Cytopro Cytocentrifuge; ELITech Group, Logan, UT, USA) stained with DiffQuick (Siemens, Newark, DE, USA). From cell-free supernate of the first lavage fraction, TNF-α, IL-6, and murine neutrophil chemokines, CXCL1 and CXCL2, were quantitated by ELISA (R&D Systems, Minneapolis, MN, USA) as they have been implicated in agriculture exposure-induced lung inflammation[21,36,37] with limits of detectability of 7.2, 1.8, 2.0, and 1.5 pg/mL, respectively. Amphiregulin (AREG; regulates fibrosis and wound repair) was quantified by ELISA (R&D Systems; limit of detectability of 12.5 pg/mL).

Histopathology

Following μCT imaging, formalin-fixed hind limbs were decalcified using 15% EDTA/0.5% paraformaldehyde in PBS at pH 8.0 for 3 weeks, changing buffer every 2 days.[34] Following decalcification, limbs were paraffin-embedded, sectioned (4 to 5 μm), and stained with modified Masson's trichrome to investigate collagen deposition. Slides were scanned with an iScan Coreo Au (Ventana, Tucson, AZ, USA) slide scanner by the institution's (University of Nebraska Medical Center) tissue sciences facility and converted into digital format. Quantification of collagen was done using Image J software (NIH, Bethesda, MD, USA; https://imagej.nih.gov/ij/; 1997 to 2016) after deconvolution and thresholding using methods previously described.[31] Next, in all experimental runs, the right half of the lungs were excised and inflated to 15-cm H_2O pressure with 10% formalin (Fisher Scientific, Fair Lawn, NJ, USA) for 24 hours to preserve pulmonary architecture.[21] Sectioned (4 to 5 μm) lungs were H&E stained, and semiquantitatively assessed for the degree and distribution of lung inflammation utilizing a modification of a previously published scoring system.[21] This scoring system evaluates the spectrum of inflammatory changes for alveolar and bronchiolar compartment inflammation, whereby each parameter was independently assigned a value from 0 to 3. The number of intrapulmonary lymphoid aggregates per section was enumerated. Lung sections were also stained with modified Masson's trichrome; collagen was quantified by ImageJ as described above.

Lung cell staining and flow cytometry

In one experimental run, the left side of the lungs was harvested after perfusion and subjected to an automated dissociation procedure using a gentleMACS Dissociator instrument (Miltenyi Biotech, Auburn, CA, USA).[22] Viability of the final cell preparation or "total lung cells" was assessed by trypan blue exclusion and a LIVE/DEAD Fixable Blue Dead Cell Stain Kit (Invitrogen, Carlsbad, CA, USA). Ultimately, $< 1\%$ of gated cells were not viable, with no difference by treatment group (not shown). Lung cells from each animal were incubated with CD16/32 (Fc Block, BD Biosciences, San Jose, CA, USA) to minimize nonspecific antibody staining, then stained with mAbs directed against rat anti-mouse CD45 (clone: 30-F11), CD11b (clone: M1/70), Ly6G (clone 1A8), CD4 (clone RM 4 to 5), CD8 (clone: 53 to 6.7), and hamster anti-mouse CD3 (clone: 145-2C11), and rat anti-mouse CD19 (clone: eBio1D3) and CD11c (clone: N418). Antibodies to CD45 and CD19 were obtained from eBioscience (Santa Clara, CA, USA); CD11b and Ly6G from BioLegend (San Diego, CA, USA), CD11c from Invitrogen, and the remainder from BD Biosciences. Gating strategies for $CD11c^+CD11b^{lo}$ alveolar macrophages, $CD11c^+CD11b^{hi}$ exudate macrophages, $Ly6G^+$ neutrophils, $CD3^+CD4^+$ and $CD3^+CD8^+$ T cells, and $CD3^-CD19^+$ B cells were previously reported.[38] The percentage of all respective cell populations was determined from live $CD45^+$ lung leukocytes after excluding debris and doublets. This percentage was multiplied by the respective total lung cell numbers to determine specific cell population numbers for each animal.

Lung hyaluronan and fibronectin analysis

Hyaluronan and fibronectin, markers of extracellular lung matrix involved in fibrosis, were characterized. In a separate experimental run, the left side of the lungs was prepared by homogenizing lung tissue in 500 μl of sterile PBS, and levels were determined from cell-free homogenates according to manufacturer's recommendation using ELISA kits for hyaluronan (Echelon Biosciences, Salt Lake City, UT, USA) and fibronectin (Abcam, Cambridge, MA, USA), with a lower limit of detection of 12.5 and 3 ng/mL, respectively. AREG was also quantified on lung homogenates as described for BALF.

Serum

Serum from whole blood was collected and pentraxin-2 (murine acute phase reactant protein) levels were quantified by quantikine ELISA according to manufacturer's instructions (R&D Systems). Anti-MAA antibodies (IgG) were quantified as previously described.[22] Anticitrullinated peptide antigen (ACPA) was determined using a modification of the second-generation anti-CCP antibody ELISA (Diastat; Axis-Shield Diagnostics, Dundee, UK) as previously described.[30] Concentrations of antibody to mouse type II collagen was determined using ELISA-grade mouse type II collagen as the coating antigen (Chondrex) and detected using an HRP-conjugated goat antimouse antibody specific for IgG (Fcγ-specific; Jackson

ImmunoResearch, West Grove, PA, USA). Total serum IgM, IgA, and IgG were quantified according to manufacturer's instruction using a Quantikine Enzyme-Linked Immunosorbent Assay Kit (Affymetrix eBioscience, Santa Clara, CA, USA).

Statistical methods

Sample-size calculation was estimated from a previous unrelated study in nonarthritis C57BL/6 male mice exposed to inhalant endotoxin,[39] whereby we calculated a sample size of $n = 4$ in each group, to achieve 80% power at the 0.05 level of significance to detect a difference in BMD (g/mm^3), assuming a mean (SD) of 0.22 (0.02) for the control group and a mean (SD) of 0.18 (0.02) for the exposed group. Experimental groups were run with five mice per each group. We ran two independent experimental runs for the male mice, and one run for the female mice. One male mouse in the arthritis group (CIA) died during isoflurane inhalation at week 2. Thus, the total maximum possible is $N = 9$ CIA male mice and $N = 10$ sham, ODE, and CIA + ODE mice/group from two independent studies ($N = 39$ total male mice), and $N = 5$ female mice/group ($N = 20$ total female mice). Arthritis scores, bones, lavage fluid, lung histology, and serum were collected on all mice. Lungs were divided into right side and left side. The right side of the lungs were used for histology and the left side of the lungs were either processed for flow cytometry ($N = 4$ CIA mice and $N = 5$ sham, ODE, and CIA + ODE mice/group) or homogenized ($N = 5$ mice/group). Numbers less than 9 to 10 reflect limitations in available sample quantity or quality.

Data are presented as the mean ± SEM. To detect significant changes among three or more groups, an ANOVA was utilized and a post hoc test (Tukey/LSD) or nonparametric Mann-Whitney test was performed to account for multiple comparisons if the p value was < 0.05. All statistical analyses were performed using the GraphPad Prism software, version 7.03 (GraphPad, San Diego, CA, USA) and statistical significance accepted at $p < 0.05$.

Results

Arthritis inflammatory scores

Throughout the 5-week experiment, the highest arthritis inflammatory scores were demonstrated for CIA + ODE (Fig. 1*A*) male mice. Arthritis inflammatory scores were increased in CIA + ODE, CIA, and ODE as compared with sham beginning at 3 weeks. CIA + ODE and CIA treatment groups demonstrated significantly increased inflammatory scores at 5 weeks as compared with ODE alone ($p < 0.05$). There was no significant difference in inflammatory scores between CIA + ODE and CIA.

Bone loss

μCT imaging demonstrated that CIA and CIA + ODE resulted in significant trabecular bone loss (Fig. 1*B*, image) in the same male mice. Trabecular bone parameters for the proximal tibia and calcaneus for the four male groups were normalized to

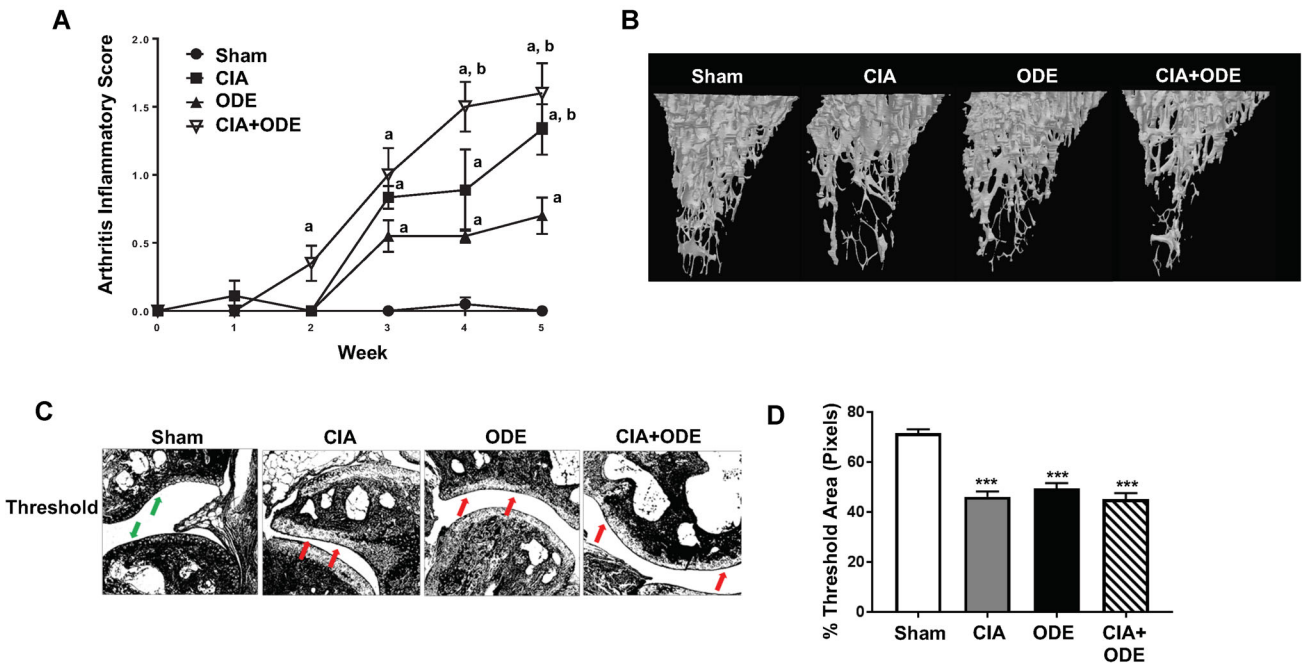

Fig. 1. Organic dust extract (ODE) exposure potentiates collagen-induced arthritis (CIA) and bone/joint disease in male mice. (*A*) Line graph depicts mean with SE bars of arthritis inflammatory score at respective time points from treatment groups. Statistical difference versus sham denoted as "a" ($p < 0.05$); versus ODE denoted as "b" ($p < 0.05$). $N = 9$ CIA mice and $N = 10$ sham, ODE, CIA + ODE mice/group from two independent studies. (*B*) A representative 3D reconstructed image from region of interest of proximal tibia from one mouse per treatment group. Note the loss trabecular bone in the CIA and further loss in the CIA + ODE treatment groups as compared with sham. (*C*) Representative image from each treatment group of ankle sections stained for collagen using Masson's trichrome and thresholding performed. Green arrows indicate areas of a normal joint tissue with increased presence of collagen. Red arrows indicate areas of articular cartilage loss in the CIA, ODE, and CIA + ODE groups compared with controls. A significant decrease (***$p < 0.001$ versus sham) in collagen observed when images converted to pixels using ImageJ (*D*)

sham control to account for differences among experimental runs and are shown in Table 1. As compared with sham, CIA resulted in declines in BMD (–17%), bone volume (–15%), and trabecular number (–14%) in the proximal tibia with increases in trabecular separation (+ 10%) and trabecular pattern factor (+ 10%). In the calcaneus, CIA mice demonstrated reduced BMD (–10%) and trabecular number (–10%) as compared with sham. Next, combination of CIA + ODE resulted in reductions in BMD (–31%), bone volume (–26%), trabecular number (–27%), and polar moment of inertia (–18%), with a corresponding increase in trabecular separation (+ 21%) and trabecular pattern factor (+ 18%) in the proximal tibia as compared with sham. Similar patterns of bone deterioration in the calcaneus were demonstrated for BMD (–25%), bone volume (–23%), specific bone surface area (+ 15%), trabecular thickness (–13%), trabecular number (–18%), trabecular pattern factor (+ 31%), and polar moment of inertia (–36%). Whereas there were no significant changes found in bone parameters with ODE alone, ODE significantly potentiated several, but not all, parameters related to arthritis-associated deterioration of bone quantity and quality in the tibia and calcaneus (Table 1). Namely, there were three significant ($p < 0.05$) bone parameter differences between CIA and CIA + ODE in the tibia that included differences in BMD, trabecular number, and trabecular separation. In the calcaneus, there were six significant differences between CIA and CIA + ODE that included BMD, bone volume, specific bone surface area, trabecular thickness, trabecular separation, and polar moment of inertia (Table 1).

Collagen staining

Collagen staining with thresholding demonstrated articular cartilage loss in CIA, ODE, and CIA+ODE compared with sham (Fig. 1*C*). This was confirmed using ImageJ quantification showing a significant decrease ($p < 0.001$) in pixels at the end of the bone in all three groups as compared with sham (Fig. 1*D*). There was no statistical difference among CIA, ODE, and CIA + ODE.

Airway inflammation

ODE exposure induced increases in BALF total cells, neutrophils, and macrophages as well as inflammatory cytokines/chemokines compared with sham (Fig. 2*A*) in same male mice. In contrast to the joint/bone findings, in CIA + ODE, airway inflammatory cell influx was reduced compared with ODE (Fig. 2*A*). ODE-induced TNF-α, IL-6, and neutrophil chemoattractants (CXCL1 and CXCL2) were also reduced in BALF from CIA + ODE animals compared with ODE (Fig. 2*B*). The epidermal growth factor agonist, amphiregulin (AREG) was elevated in ODE-treated mice as compared with sham, but reduced in CIA + ODE as compared with ODE (Fig. 2*B*). There were no increases in airway cell influx and cytokine/chemokine levels in CIA versus sham. Next, ODE induced the greatest magnitude of lung neutrophil, alveolar macrophage ($CD11c^{+}CD11b^{lo}$), exudative macrophage ($CD11c^{+}CD11b^{hi}$), and B1 B ($CD19^{+}CD11b^{+}$) cell influx of the four experimental groups (Fig. 2*C*). There were also increases in lung neutrophils and exudative macrophages in the CIA + ODE group compared with sham (Fig. 2*C*). Interestingly, there was also an increase in exudative macrophages in the CIA versus sham (Fig. 2*C*).

Lung histology and expression of extracellular matrix proteins

Lung histology demonstrated increases in the development of lymphoid aggregates and bronchiolar and alveolar inflammation in ODE and CIA + ODE compared with sham (Fig. 3*A*). By semiquantitative assessment, there were significantly ($p < 0.01$) fewer cellular aggregates and trends ($p = 0.066$) towards less inflammation in the alveolar compartment in CIA + ODE compared with ODE. CIA did not induce significant changes in

Table 1. Trabecular Bone Parameters by Treatment Group in Male Mice

	Sham	CIA	ODE	CIA + ODE
Proximal tibia				
BMD	1.00 ± 0.04	0.83 ± 0.03*	1.00 ± 0.04	0.69 ± 0.05***#
Bone volume	1.00 ± 0.03	0.85 ± 0.04*	0.99 ± 0.03	0.74 ± 0.05***
Specific bone surface area	1.00 ± 0.01	1.03 ± 0.01	1.01 ± 0.01	1.06 ± 0.04
Trabecular thickness	1.00 ± 0.01	0.97 ± 0.02	0.98 ± 0.03	0.96 ± 0.03
Trabecular number	1.00 ± 0.03	0.86 ± 0.05*	0.99 ± 0.03	0.73 ± 0.03***#
Trabecular separation	1.00 ± 0.02	1.10 ± 0.04*	0.97 ± 0.02	1.21 ± 0.03***#
Trabecular pattern factor	1.00 ± 0.01	1.10 ± 0.02*	1.05 ± 0.3	1.18 ± 0.05**
Polar moment of inertia	1.00 ± 0.06	0.93 ± 0.07	0.96 ± 0.09	0.82 ± 0.03
Calcaneus				
BMD	1.00 ± 0.02	0.90 ± 0.03*	0.94 ± 0.04	0.75 ± 0.07**#
Bone volume	1.00 ± 0.02	0.95 ± 0.03	0.96 ± 0.03	0.77 ± 0.06*##
Specific bone surface area	1.00 ± 0.02	0.95 ± 0.02	0.97 ± 0.02	1.15 ± 0.06*##
Trabecular thickness	1.00 ± 0.01	1.00 ± 0.02	0.99 ± 0.02	0.87 ± 0.35***##
Trabecular number	1.00 ± 0.02	0.90 ± 0.02*	0.93 ± 0.02	0.82 ± 0.06**
Trabecular separation	1.00 ± 0.01	1.05 ± 0.02	1.03 ± 0.03	1.17 ± 0.05#
Trabecular pattern factor	1.00 ± 0.05	1.09 ± 0.04	1.02 ± 0.04	1.31 ± 0.08*
Polar moment of inertia	1.00 ± 0.03	0.91 ± 0.07	0.95 ± 0.07	0.64 ± 0.06**##

Data represent the difference induced by treatments divided by sham as complied from two independent studies (Total $N = 9$ CIA mice and $N = 10$ sham, ODE, CIA + ODE male mice/group). Statistical difference versus sham denoted (*$p < 0.05$, **$p < 0.01$, ***$p < 0.001$); statistical difference between CIA + ODE and CIA denoted (#$p < 0.05$, ##$p < 0.01$).

Sham = saline injection/saline inhalation; ODE = Organic dust extract; CIA = collagen-induced arthritis.

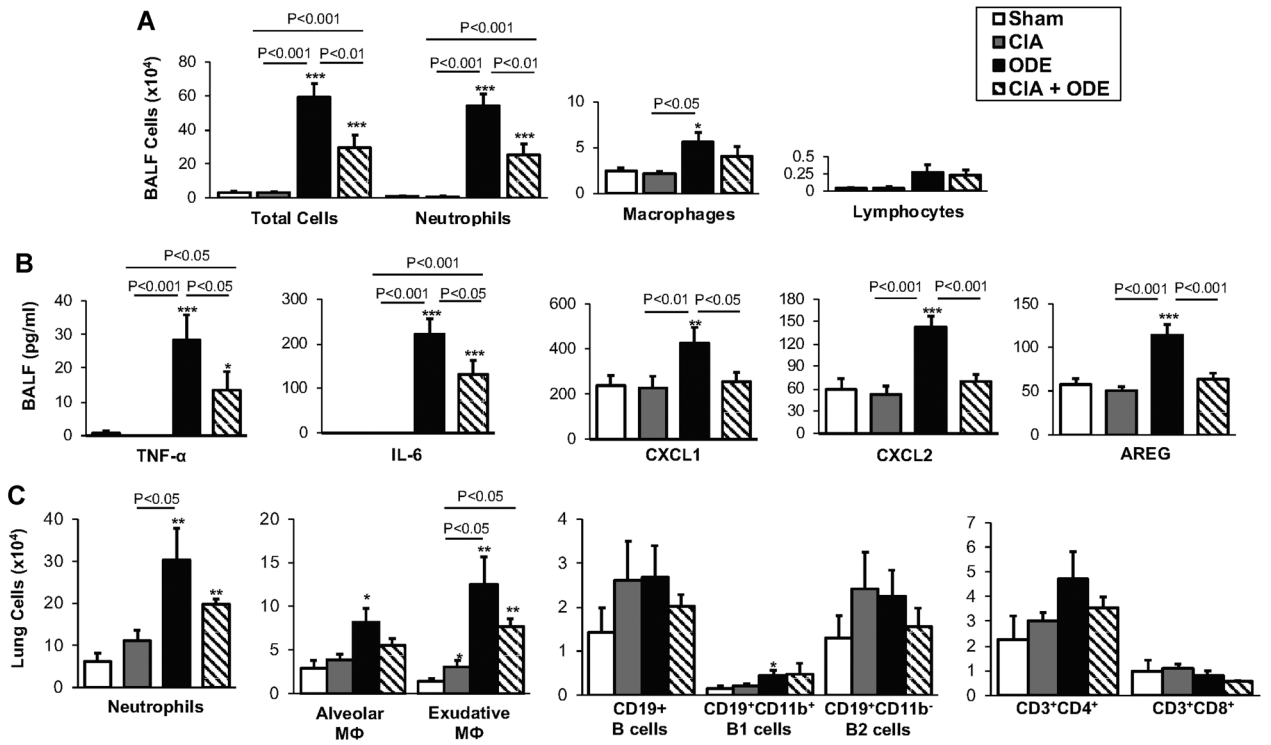

Fig. 2. Organic dust extract- (ODE-) induced airway inflammatory cell influx and mediator release is reduced in the setting of collagen-induced arthritis (CIA) in male mice. Bar graphs depict mean with SE bars of cells and mediators from treatment groups. (*A*) Total cells, neutrophils, macrophages, and lymphocytes enumerated from bronchoalveolar lavage fluid (BALF). Eosinophils were not detected. (*B*) TNF-α, IL-6, murine neutrophils chemoattractants (CXCL1 and CXCL2), and amphiregulin (AREG) levels determined by ELISA. $N = 9$ CIA mice and $N = 10$ sham, ODE, CIA + ODE mice/group from two independent studies. (*C*) Numbers of neutrophils ($Ly6G^+$), alveolar macrophages ($CD11c^{hi}CD11b^{lo}$), exudative macrophages ($CD11c^{hi}CD11b^{hi}$), B cells ($CD19^+$), and B1 ($CD19^+CD11b^+$), B1a ($CD19^+CD11b^+CD5^+$), and B2 ($CD19^+CD11b^-$) B-cell subsets from ½ whole-lung tissue cells were calculated by multiplying the % cells in respective gate (% $CD45^+$ cells, as analyzed by FACS) multiplied by respective total cells for each mouse. $N = 4$ CIA mice. $N = 5$ sham, ODE, CIA + ODE mice/group. Statistical difference (*$p < 0.05$, **$p < 0.01$, ***$p < 0.001$) versus sham or as indicated

these parameters compared with sham. There was also increased collagen staining (blue; Masson's trichrome) in ODE and CIA + ODE compared with sham by microscopic review (Fig. 3*C*); quantification by ImageJ confirmed these observations (Fig. 3*D*). Next, lung tissue homogenates were investigated for hyaluronan, fibronectin, and AREG. Compared with sham, hyaluronan was significantly increased only in CIA + ODE (Fig. 3*E*). Fibronectin levels were increased in ODE and CIA + ODE, with an augmented (nonsignificant) response in CIA + ODE versus ODE. Lung AREG levels were increased in ODE and CIA + ODE compared with sham (Fig. 3*E*) with no significant difference between these two groups.

Systemic inflammatory and autoantibody responses

Serum pentraxin-2 concentrations were increased in CIA, ODE, and CIA + ODE with the highest concentrations observed CIA + ODE (Fig. 4) in the same male mice. Serum cyclic citrullinated peptide (CCP) IgG antibody response was increased only in the CIA + ODE mice as compared with sham and CIA. The serum mouse type II collagen IgG response was increased in the CIA and CIA + ODE with no difference between groups, confirming CIA induction. Anti-MAA IgG antibody was increased ($p < 0.01$) in ODE and CIA + ODE. Serum immunoglobulin (IgG, IgM, IgA) levels are shown in Fig. 4, with increasing levels demonstrated for CIA + ODE > ODE > CIA as compared with sham. IgM and IgA levels were increased in ODE and CIA + ODE as compared with sham.

Joint/bone, lung, and systemic responses in female DBA/1J mice

In subsequent studies, female DBA/1J mice of the same age as male mice were assigned to the same experimental conditions. There was an overall reduction in the magnitude of the inflammatory arthritis, bone deterioration, and airway inflammatory responses in the female mice, predominately within the CIA + ODE; these differences are given in Table 2. The experimental endpoints in female mice that did not differ from those in male mice are shown in Supplemental Table S1. Collectively, the arthritis inflammatory scores in the female mice over the 5-week exposure period in CIA, ODE, and CIA + ODE showed nonsignificant increases as compared with sham with the exception at week 1, whereby ODE and CIA + ODE showed significant increases. There was also no significant BMD loss among exposure groups. However, there were significant ($p < 0.05$) changes in CIA versus sham for bone volume (–28%; Supplemental Table S1), specific bone surface area (+ 7%;

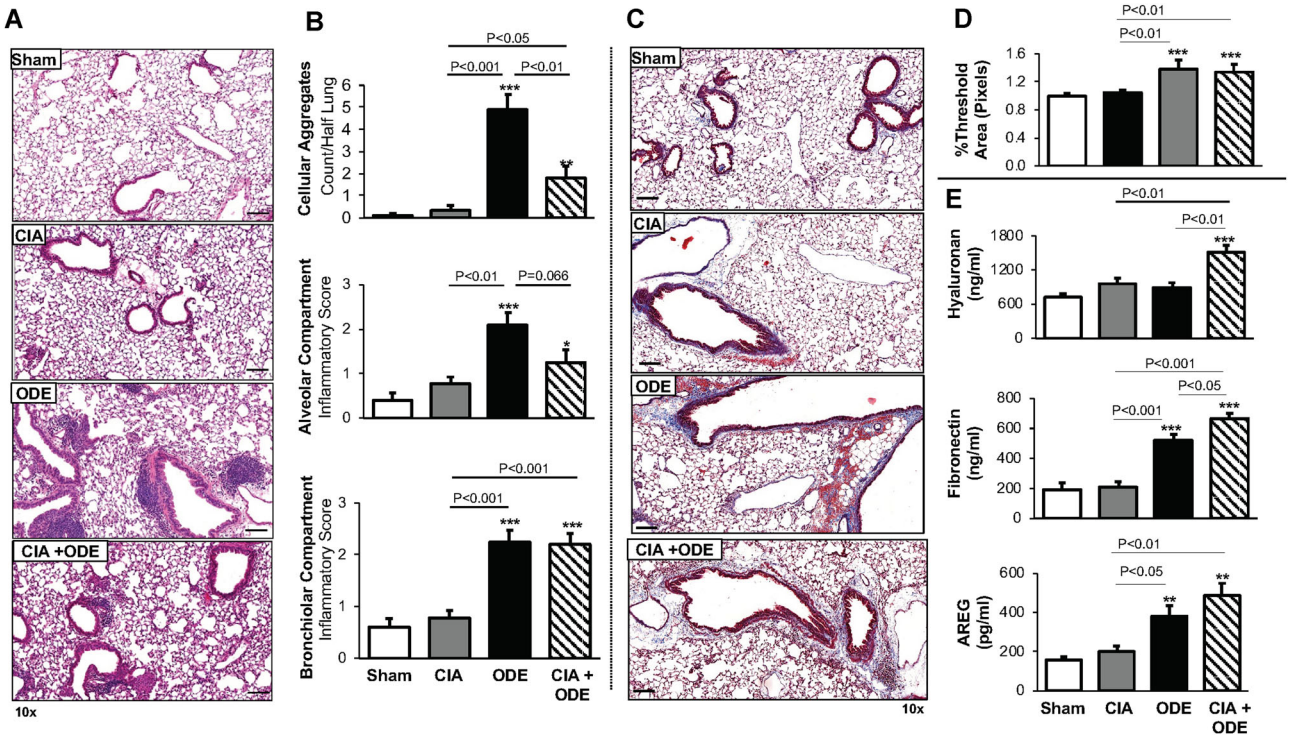

Fig. 3. Organic dust extract- (ODE-) induced lung pathology is altered in the setting of collagen-induced arthritis (CIA) in male mice. All bar graphs depict mean with SE bars. (*A*) A representative (4 to 5 μm thick) H&E-stained lung section of one mouse per treatment group. (*B*) ODE-induced cellular aggregate numbers and semiquantitative inflammatory scores of alveolar and bronchiolar compartment inflammation. $N = 9$ CIA mice and $N = 10$ sham, ODE, CIA + ODE mice/group from two independent studies. (*C* panel) A representative Masson's trichrome- (collagen = blue) stained section for each treatment group. (*D*) Increased collagen staining in ODE and CIA + ODE when images converted to pixels using imageJ analysis ($N = 5$ images/mouse; 4 mice/group). (*E*) Levels of hyaluronan, fibronectin, and amphiregulin (AREG) from left-side lung homogenates shown. $N = 5$ mice/group. Statistically significant ($^*p < 0.05$, $^{**}p < 0.01$, $^{***}p < 0.001$) versus saline or as indicated. Images shown at 10× magnification with line scale of 100 μm. ODE-induced lung parenchymal cellular aggregates and alveolar compartment inflammation were reduced in the setting of arthritis. However, collagen, lung hyaluronan, fibronectin, and amphiregulin remained elevated with combined CIA + ODE exposures

Supplemental Table S1), trabecular thickness (–8%; Supplemental Table S1), trabecular number (–22%; Table 2), trabecular separation (+ 23%; Supplemental Table S1), and polar moment of inertia (–21%; Table 2). Female mice were susceptible to ODE-induced airway inflammatory changes, and there were nonsignificant trends toward suppressed inflammatory cell influx and mediator release in CIA + ODE as compared with ODE. Serum studies revealed that pentraxin-2, CCP peptide antibody, and anticollagen type II antibody were elevated in CIA and CIA + ODE treated mice with no difference between these two groups. Anti-MAA antibodies were also elevated in ODE alone.

Discussion

In this study we demonstrated that repetitive inhalation exposures to organic dust enhance arthritis and bone deterioration with a corresponding increase in systemic inflammation and production of IgG anti-CCP antibody in arthritis prone, DBA/1J male mice. In these same mice, coexposure with CIA and ODE led to a suppression of ODE-induced airway neutrophilic inflammation with a potential shift toward interstitial lung disease processes based upon increased extracellular matrix protein deposition. These collective findings were not consistently demonstrated with female mice: This underscores the importance of biological sex differences in animal modeling strategies. These sex differences appear to correspond to epidemiological observations, whereby occupational exposures, such as farming exposures, are increasingly recognized as risk factors for RA and related morbidity in men as opposed to women.[17] Further exploitation of this animal model to understand the joint/bone-lung inflammation connection to study mechanisms and test preventative and/or therapeutic strategies could be of utility.

Occupational exposures including farming, construction, mechanics, and warehouse work have been implicated in increasing RA development and RA morbidity in men.[17] In support of these epidemiologic observations, our studies demonstrated enhanced arthritis and related bone damage in inhalant ODE-treated male mice subjected to arthritis induction. Of the articular/bone experimental endpoints, bone loss and deterioration were most pronounced with coexposure. Articular collagen loss was similar among the three exposure groups with no potentiation observed with coexposure. However, there was an incremental, but nonsignificant, increase in the arthritis inflammatory score with coexposure. These data suggest that repetitive inhalant exposure to a

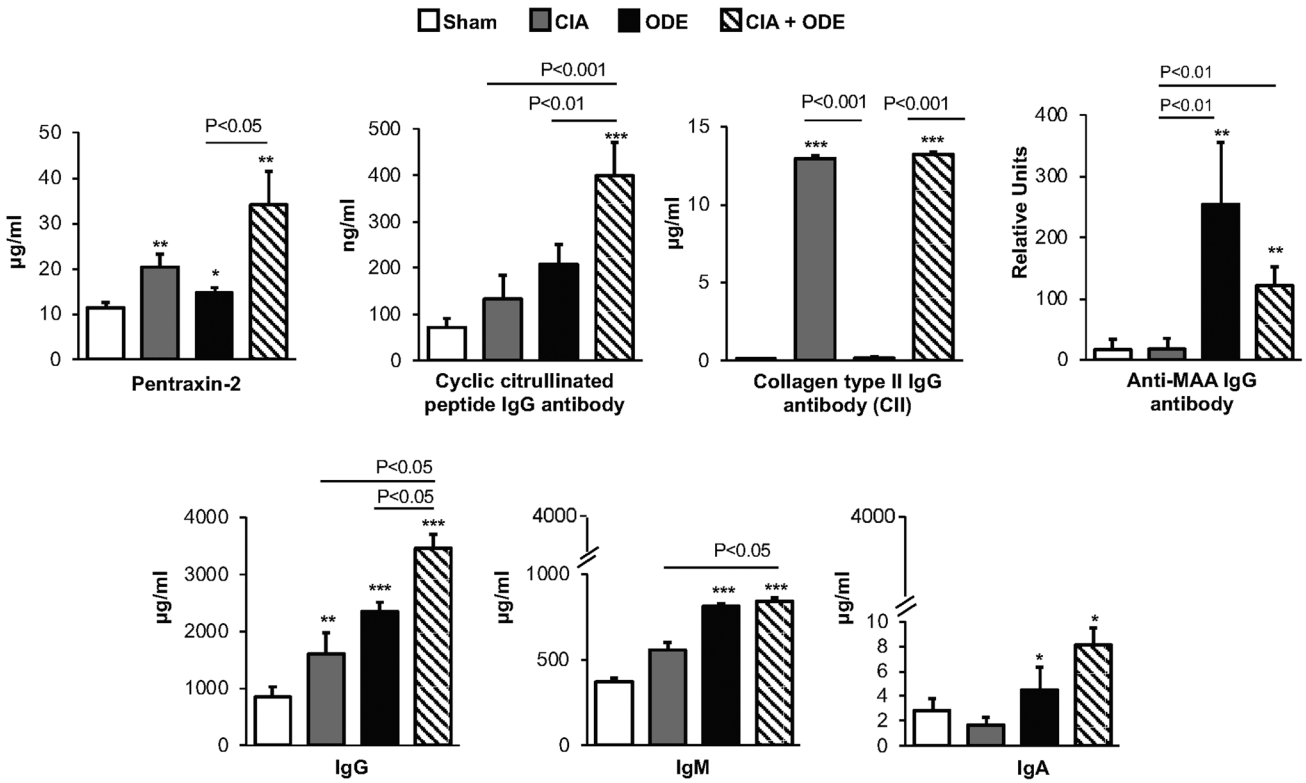

Fig. 4. Serum levels of biomarkers, autoreactive IgG antibodies, and immunoglobulins varied by treatment group in male mice. Bar graphs depict mean with SE bars. Serum levels of the acute-phase reactant protein pentraxin-2, cyclic citrullinated peptide IgG antibody, collagen type II IgG antibody (CII), and anti-MAA IgG antibody, IgG, IgM, and IgA as determined by ELISA. Statistical difference versus sham (*$p < 0.05$, **$p < 0.01$, **$p < 0.001$) and between groups as noted by lines. $N = 9$ CIA mice and $N = 10$ sham, ODE, CIA+ODE mice/group from two independent studies

complex, microbial-enriched inflammatory agent can induce articular disease alone, but importantly, may potentiate arthritis. Thus, for the occupational worker, these findings suggest that respiratory protection should be encouraged in persons with RA regularly exposed to environmental pollutants, as such inhalant exposures could worsen RA disease.

Consistent with articular/bone findings, serum studies demonstrated that coexposure (CIA + ODE) was associated with the greatest levels of pentraxin-2, a murine acute-phase reactant protein, and strikingly, high levels of anti-CCP antibody. In previous work, we found that inhalant ODE treatment increased the airway expression of citrullinated and MAA-modified proteins; in addition, we observed low-grade anti-CCP and anti-MAA antibody responses in C57BL/6 mice.[22] In these studies with the arthritis-susceptible DBA/1J mice, anti-CCP antibody responses were strikingly augmented in CIA + ODE treated mice. These studies strongly support that inhalant exposure to inflammatory environmental agents can potentiate articular bone and systemic autoreactive disease.

Surprisingly, airway inflammation characterized by neutrophil influx, inflammatory cytokine/chemokine release, and the formation of cellular aggregates were not potentiated with coexposure. In contrast to the augmented bone and systemic response with coexposure, male mice treated with arthritis induction during ODE inhalant exposure had less evidence of airway inflammation. Because it is recognized that there is a balance between lung inflammatory and tissue remodeling processes, we investigated mediators implicated in remodeling. The data support a potential balance shift with the coexposure modeling towards interstitial disease because collagen deposition and tissue levels of extracellular matrix proteins (ie, hyaluronan and fibronectin) remained elevated or augmented in the setting of CIA + ODE despite decreased levels of the classic inflammatory mediators. AREG has been characterized as both protective and injurious in the progression of various lung diseases as it can promote proresolution effector cell function and epithelial repair processes, but overexpression can lead to fibrotic remodeling.[40,41] Amphiregulin remained elevated with coexposure in the lung tissues, which is interpreted to be supportive of evidence towards interstitial disease. Macrophages have also been implicated in promoting lung fibrosis.[42] Moreover, others have shown that the elimination of $CD11b^{hi}$ macrophages protects mice from bleomycin-induced fibrosis.[43] Interestingly, there was evidence that arthritis induction alone impacted the lung environment as CIA increased activated lung $CD11c^{+}CD11b^{hi}$ macrophages that could work to modulate lung inflammation. Conversely, pulmonary fibrosis is a pathology that can be exacerbated by the function of anti-inflammatory macrophages; a reduction in activated macrophages was demonstrated in these coexposed mice. Thus, it is possible that systemic arthritis induction skews the lung immune response towards interstitial lung disease processes and that targeting macrophage function could be a potential strategy to modulate RA–lung disease.

Table 2. Experimental Endpoints in Female Mice That Differed With Those in Male Mice[1]

	Sham	CIA	ODE	CIA + ODE	
	(a)	(b)	(c)	(d)	Versus male mice[3]
Arthritis score: Week 1	0.0 ± 0.0	0.2 ± 0.12	0.7 ± 0.12**	0.6 ± 0.19*	c↑, d↑
Arthritis score: Week 3	0.0 ± 0.0	0.4 ± 0.19	0.4 ± 0.19	0.2 ± 0.12	d↓
Arthritis score: Week 4	0.0 ± 0.0	0.5 ± 0.35	0.5 ± 0.22	0.3 ± 0.12	d↓
Arthritis score: Week 5	0.0 ± 0.0	0.5 ± 0.29	0.2 ± 0.2	0.2 ± 0.2	d↓
BMD[2]	1.00 ± 0.01	1.03 ± 0.01	0.98 ±0 0.02	1.01 ± 0.01	b↑, d↑
Trabecular number[2]	1.00 ± 0.03	0.78 ± 0.08*	1.05 ± 0.10	0.951± 0.08	d↑
Polar moment of inertia[2]	1.00 ± 0.04	0.79 ± 0.07*	1.06 ± 0.13	1.05 ± 0.16	d↑
BALF TNF-α (pg/mL)	0.0 ± 0.0	0.6 ± 0.4	15.9 ± 9.9**,#	0.1 ± 0.1	c↓,d↓
BALF IL-6 (pg/ml)	0.3 ± 03	0.4 ± 0.4	213.6 ± 80.0**	101.7 ± 34.0*	c↓,d↓
BALF CXCL1 (pg/mL)	0.1 ± 0.1	155.7 ± 51.4*	274.1 ± 67.4*	139.5 ± 19.0*	c↓
BALF CXCL2 (pg/mL)	0.0 ± 0.0	50.7 ± 12.4**	69.6 ± 23.3**	29.1 ± 5.8**	c↓,d↓
Lung hyaluronan (ng/mL)	473 ± 6	624 ± 47*	895 ± 113**,^	864 ± 44**,^	a↓,d↓
Lung Fibronectin (ng/mL)	223 ± 27	317 ± 88	277 ±31	397 ± 21**	c↓,d↓
Lung amphiregulin (pg/mL)	170 ± 19	12 ± 12*	501 ± 70***,^^	242 ± 36	b↓, d↓
Bronchiolar lung score	0.0 ± 0.0	0.25 ± 0.25	1.25 ± 0.25**	1.0 ± 0.3*	d↓
CCP IgG (ng/mL)	62.5 ± 6.2	347.3 ± 44.53*	30.35 ± 22.19^^	388.4 ± 125.5*	b↑,c↓
Collagen type II ab (μg/mL)	0.05 ± 0.04	6.3 ± 3.3**	0.035 ± 0.019	7.6 ± 0.77**	b↓,d↓
Anti-MAA (Rel units)	110.6 ± 46.3	991 ± 366**	343.5 ± 40.05^	518.5 ± 104.1	b↑,c↑,d↑

Sham = saline injection/saline inhalation; ODE = Organic dust extract; CIA = collagen-induced arthritis; BALF = bronchoalveolar lavage fluid; MAA = malondialdehyde-acetaldehyde.

[1]Statistical difference versus sham denoted (*$p < 0.05$, **$p < 0.01$); between ODE and CIA + ODE denoted (##$p < 0.01$); vs. CIA denoted (^$p < 0.05$ and ^^$p < 0.01$). $N = 5$ female mice/group.

[2]Data represent the difference induced by treatments divided by sham of proximal tibia.

[3]Statistical differences between females versus males of same exposure denoted with letter when $p < 0.05$ for sham (a), CIA (b), ODE (c), and CIA + ODE (d) groups and arrow represents direction of difference of female findings as compared to males.

With renewed emphasis for transparent reporting in animal modeling studies,[44] separate studies were conducted with female mice, and the sex differences demonstrated in this study could have implications for future studies. We found that joint and bone damage in female mice subjected to CIA were attenuated relative to male mice, and inhalant ODE exposures had no significant impact on these parameters as it did in the male mice. Although airway inflammation was increased in female mice following ODE and this response was slightly dampened in the setting of arthritis, these findings were less striking than those observed in male mice. In contrast to male mice, increases in systemic inflammation and autoantibody responses were demonstrated in CIA and CIA + ODE, but not in ODE-exposed female mice. These striking differences would strongly implicate roles for sex hormones in regulating the arthritis/bone–lung inflammatory axis. These findings were also consistent with previous work in C57BL/6 animals demonstrating that female mice were protected against inhalant endotoxin-induced bone loss, whereas oophorectomized female mice were highly susceptible.[39] Furthermore, in studies done by others with SKG mice investigating RA-associated ILD, only female mice were utilized.[20] In those female animal studies, there was also a lack of arthritis development following cigarette smoke exposure or bleomycin-induced lung injury.[20] Thus, our studies shed further light on the complex relationship underlying how inhalant exposures might impact arthritis in a sex-dependent fashion. Importantly, future studies could manipulate various sex hormones (ie, testosterone, progesterone, estrogen) to determine specific effects on the development and progression of arthritis and lung disease.

There are several limitations of this study. First, the induction of arthritis and environmental inhalant exposure were conducted simultaneously, and it would clearly be informative to stagger the timing of environmental inhalant exposure to either before or after arthritis induction. The former may be particularly important because the prevalence of subclinical lung disease in RA is variable and ranges from 19% to 57%.[45] Although the overall degree of arthritis was mild, the impact of coexposures on bone quantity and quality was significant, which highlights that lung inflammation in RA leads to increased articular inflammation, bone destruction, and cartilage erosion. Next, bone loss and destruction in RA can be induced through the activation of osteoclasts from inflammatory processes or a disruption in osteoblast/osteoclast balance. Thus, future studies investigating osteoclast precursors, osteoclasts, osteoblast activity, and osteocytes may be warranted in these coexposure settings. In addition, serial joint imaging using live animal imaging modalities could be advantageous to further quantify changes in a temporal manner. Investigations utilizing organic dust from various agricultural and occupational settings should be explored. Finally, it is important to recognize that this model induces airway inflammation as opposed to emphysematous changes.

In summary, the link between arthritis and lung inflammatory disease is further strengthened with this novel animal model that strongly supports that repetitive inhalant exposure to an environmental inflammatory agent influences and potentiates systemic autoimmunity, articular disease, and bone loss. In converse, arthritis induction appears to modulate the lung immune response to inhalant exposures to impact the inflammatory/interstitial lung processes. Occupational

exposures are increasingly implicated in the development and severity of RA in men, and this preclinical animal model could be further exploited to understand these relationships to develop strategies to mitigate arthritis and lung disease for at-risk individuals.

Disclosures

All authors have no disclosures.

Acknowledgments

This study was supported by grants from the National Institute of Environmental Health Sciences (R01ES019325 to JAP) and the National Institute for Occupational Safety and Health (U54OH010162 to JAP). This study was supported in part by the Central States Center for Agricultural Safety and Health (CS-CASH). TRM is supported by a VA Merit Award (CX000896) and grants from the National Institute of General Medical Sciences (U54GM115458) and the National Institute on Alcohol Abuse and Alcoholism (R25AA020818). The study was also supported by the Fred & Pamela Buffett Cancer Center (Flow Cytometry Research Facility and Tissue Sciences Facility) Shared Resource, supported by the National Cancer Institute under award number P30CA036727.

The authors acknowledge members of the Tissue Sciences Facility at the Department of Pathology and Microbiology (University of Nebraska Medical Center, Omaha, NE, USA) for assistance with tissue processing and staining. We thank Janice A Taylor and James R Talaska of the Advanced Microscopy Core Facility at the University of Nebraska Medical Center for providing assistance with (confocal or super resolution) microscopy. We acknowledge members of the Experimental Immunology Laboratory including Carlos D Hunter, Karen C Easterling, Jacob D McGowan, and Logan M Duryee for their technical assistance. We thank Victoria B Smith, Samantha Wall, and Craig Semerad in the Flow Cytometry Research Core Facility at the University of Nebraska Medical Center for providing assistance with flow cytometry studies. We thank Art Heires for technical service, and Xioayan Wang and Gang Zhao for assistance with the μCT scanning and analysis.

Authors' roles: JAP, GMT, and TRM made substantial contributions to conception and design; JAP, KJ, AJN, MJD, KR, BRE, JC, DW, and BS acquired data; JAP, GMT, BRE, DJR, and TRM analyzed and interpreted the data; JAP and TRM drafted the manuscript. All authors revised it critically for important intellectual content and approved the final version of the submitted manuscript. All authors agree to be accountable for all aspects of the work in ensuring that questions related to the accuracy or integrity of any part of the work are appropriately investigated and resolved.

References

1. Erickson AR, Canella AC, Mikuls TR. Clinical features of rheumatoid arthritis. In: Budd RC, Gabriel SB, McInnes IB, & O'Dell JR, editors, *Kelley & Firestein's Textbook of Rheumatology*. 2nd ed. Philadelphia. Elsevier, 2017) 1167–86.
2. England BR, Sayles H, Michaud K, et al. Cause-specific mortality in male US veterans with rheumatoid arthritis. Arthritis Care Res (Hoboken). 2016;68:36–45.
3. Sparks JA, Chang SC, Liao KP. Rheumatoid arthritis and mortality among women during 36 years of prospective follow-up: results from the nurses' health study. Arthritis Care Res (Hoboken). 2016;68:753–62.
4. Shaw M, Collins BF, Ho LA, Raghu G. Rheumatoid arthritis-associated lung disease. Eur Respir Rev. 2015;24:1–16.
5. Olson AL, Swigris JJ, Sprunger DB, et al. Rheumatoid arthritis-interstitial lung disease-associated mortality. Am J Respir Crit Care Med. 2011;183:372–78.
6. Koduri G, Norton S, Young A, et al. Interstitial lung disease has a poor prognosis in rheumatoid arthritis: results from an inception cohort. Rheumatology (Oxford). 2010;49:1483–89.
7. Nannini C, Medina-Velasquez YF, Achenbach SJ, et al. Incidence and mortality of obstructive lung disease in rheumatoid arthritis: a population-based study. Arthritis Care Res (Hoboken). 2013;65:1243–50.
8. Rangel-Moreno J, Hartson L, Navarro C, et al. Inducible bronchus-associated lymphoid tissue (iBALT) in patients with pulmonary complications of rheumatoid arthritis. J Clin Invest. 2006;116:3183–94.
9. Gizinski AM, Mascolo M, Loucks JL, et al. Rheumatoid arthritis (RA)-specific autoantibodies in patients with interstitial lung disease and absence of clinically apparent articular RA. Clin Rheumatol. 2009;28:611–13.
10. Janssen KM, de Smit MJ, Brouwer E, et al. Rheumatoid arthritis-associated autoantibodies in non-rheumatoid arthritis patients with mucosal inflammation: a case-control study. Arthritis Res Ther. 2015;17:174.
11. Quirke AM, Perry E, Cartwright A, et al. Bronchiectasis is a model for chronic bacterial infection inducing autoimmunity in rheumatoid arthritis. Arthritis Rheumatol. 2015;67:2335–42.
12. Ruiz-Esquide V, Gomara MJ, Peinado VI, et al. Anti-citrullinated peptide antibodies in the serum of heavy smokers without rheumatoid arthritis. A differential effect of chronic obstructive pulmonary disease? Clin Rheumatol. 2012;31:1047–50.
13. Perry E, Eggleton P, De Soyza A, Hutchinson D, Kelly C. Increased disease activity, severity and autoantibody positivity in rheumatoid arthritis patients with co-existent bronchiectasis. Int J Rheum Dis. 2017;20:2003-2011.
14. Aubart F, Crestani B, Nicaise-Roland P, et al. High levels of anti-cyclic citrullinated peptide autoantibodies are associated with co-occurrence of pulmonary diseases with rheumatoid arthritis. J Rheumatol. 2011;38:979–82.
15. Anderson R, Meyer PW, Ally MM, Tikly M. Smoking and air pollution as pro-inflammatory triggers for the development of rheumatoid arthritis. Nicotine Tob Res. 2016;18:1556–65.
16. Newkirk MM, Mitchell S, Procino M, et al. Chronic smoke exposure induces rheumatoid factor and anti-heat shock protein 70 autoantibodies in susceptible mice and humans with lung disease. Eur J Immunol. 2012;42:1051–61.
17. Murphy D, Hutchinson D. Is male rheumatoid arthritis an occupational disease? A review. Open Rheumatol J. 2017;11:88–105.
18. Too CL, Muhamad NA, Ilar A, et al. Occupational exposure to textile dust increases the risk of rheumatoid arthritis: results from a Malaysian population-based case-control study. Ann Rheum Dis. 2016;75:997–1002.
19. Stolt P, Yahya A, Bengtsson C, et al. Silica exposure among male current smokers is associated with a high risk of developing ACPA-positive rheumatoid arthritis. Ann Rheum Dis. 2010;69:1072–76.
20. Keith RC, Powers JL, Redente EF, et al. A novel model of rheumatoid arthritis-associated interstitial lung disease in SKG mice. Exp Lung Res. 2012;38:55–66.
21. Poole JA, Wyatt TA, Oldenburg PJ, et al. Intranasal organic dust exposure-induced airway adaptation response marked by persistent lung inflammation and pathology in mice. Am J Physiol Lung Cell Mol Physiol. 2009;296:L1085–95.
22. Poole JA, Mikuls TR, Duryee MJ, et al. A role for B cells in organic dust induced lung inflammation. Respir Res. 2017;18:214.

23. Thiele GM, Duryee MJ, Anderson DR, et al. Malondialdehyde-acetaldehyde adducts and anti-malondialdehyde-acetaldehyde antibodies in rheumatoid arthritis. Arthritis Rheumatol. 2015;67:645–55.
24. Boissy RJ, Romberger DJ, Roughead WA, et al. Shotgun pyrosequencing metagenomic analyses of dusts from swine confinement and grain facilities. PLoS One. 2014;9:e95578.
25. Nehme B, Letourneau V, Forster RJ, Veillette M, Duchaine C. Culture-independent approach of the bacterial bioaerosol diversity in the standard swine confinement buildings, and assessment of the seasonal effect. Environ Microbiol. 2008;10:665–75.
26. Ilar A, Alfredsson L, Wiebert P, Klareskog L, Bengtsson C. Occupation and risk of developing rheumatoid arthritis: results from a population-based case-control study. Arthritis Care Res (Hoboken). 2018;70:499–509.
27. Leveque-Morlais N, Tual S, Clin B, Adjemian A, Baldi I, Lebailly P. The AGRIculture and CANcer (AGRICAN) cohort study: enrollment and causes of death for the 2005–2009 period. Int Arch Occup Environ Health. 2015;88:61–73.
28. Gold LS, Ward MH, Dosemeci M, De Roos AJ. Systemic autoimmune disease mortality and occupational exposures. Arthritis Rheum. 2007;56:3189–201.
29. Poole JA, Dooley GP, Saito R, et al. Muramic acid, endotoxin, 3-hydroxy fatty acids, and ergosterol content explain monocyte and epithelial cell inflammatory responses to agricultural dusts. J Toxicol Environ Health A. 2010;73:684–700.
30. Thiele GM, Duryee MJ, Dusad A, et al. Citrullinated mouse collagen administered to DBA/1J mice in the absence of adjuvant initiates arthritis. Int Immunopharmacol. 2012;13:424–31.
31. Dusad A, Duryee MJ, Shaw AT, et al. Induction of bone loss in DBA/1J mice immunized with citrullinated autologous mouse type II collagen in the absence of adjuvant. Immunol Res. 2014;58:51–60.
32. Poole JA, Romberger DJ, Wyatt TA, et al. Age impacts pulmonary inflammation and systemic bone response to inhaled organic dust exposure. J Toxicol Environ Health A. 2015;78(19): 1–16.
33. Monso E, Schenker M, Radon K, et al. Region-related risk factors for respiratory symptoms in European and Californian farmers. Eur Respir J. 2003;21:323–31.
34. Dusad A, Thiele GM, Klassen LW, et al. Organic dust, lipopolysaccharide, and peptidoglycan inhalant exposures result in bone loss/disease. Am J Respir Cell Mol Biol. 2013;49:829–36.
35. Dempster DW, Compston JE, Drezner MK, et al. Standardized nomenclature, symbols, and units for bone histomorphometry: a 2012 update of the report of the ASBMR Histomorphometry Nomenclature Committee. J Bone Miner Res. 2013;28:2–17.
36. Charavaryamath C, Juneau V, Suri SS, Janardhan KS, Townsend H, Singh B. Role of Toll-like receptor 4 in lung inflammation following exposure to swine barn air. Exp Lung Res. 2008;34:19–35.
37. Robbe P, Draijer C, Borg TR, et al. Distinct macrophage phenotypes in allergic and nonallergic lung inflammation. Am J Physiol Lung Cell Mol Physiol. 2015;308:L358–67.
38. Poole JA, Gleason AM, Bauer C, et al. CD11c+/CD11b+ cells are critical for organic dust-elicited murine lung inflammation. Am J Respir Cell Mol Biol. 2012;47:652–59.
39. Nelson AJ, Roy SK, Warren K, et al. Sex differences impact the lung-bone inflammatory response to repetitive inhalant lipopolysaccharide exposures in mice. J Immunotoxicol. 2018;15:73–81.
40. Berasain C, Avila MA. Amphiregulin. Semin Cell Dev Biol. 2014;28:31–41.
41. Xu Y, Meng C, Liu G, et al. Classically activated macrophages protect against lipopolysaccharide-induced acute lung injury by expressing amphiregulin in mice. Anesthesiology. 2016;124:1086–99.
42. Puttur F, Gregory LG, Lloyd CM. Airway macrophages as the guardians of tissue repair in the lung. Immunol Cell Biol. 2019;97(3):246–57.
43. McCubbrey AL, Barthel L, Mohning MP, et al. Deletion of c-FLIP from CD11b(hi) macrophages prevents development of bleomycin-induced lung fibrosis. Am J Respir Cell Mol Biol. 2018;58:66–78.
44. Landis SC, Amara SG, Asadullah K, et al. A call for transparent reporting to optimize the predictive value of preclinical research. Nature. 2012;490:187–91.
45. Spagnolo P, Lee JC, Sverzellati N, Rossi G, Cottin V. The lung in rheumatoid arthritis—focus on interstitial lung disease. Arthritis Rheumatol. 2018;70:1544–54.